

Prediction of pedestrian dynamics in complex architectures with artificial neural networks

Antoine Tordeux, Mohcine Chraibi, Armin Seyfried & Andreas Schadschneider

To cite this article: Antoine Tordeux, Mohcine Chraibi, Armin Seyfried & Andreas Schadschneider (2019): Prediction of pedestrian dynamics in complex architectures with artificial neural networks, Journal of Intelligent Transportation Systems, DOI: [10.1080/15472450.2019.1621756](https://doi.org/10.1080/15472450.2019.1621756)

To link to this article: <https://doi.org/10.1080/15472450.2019.1621756>



Published online: 04 Jun 2019.



Submit your article to this journal [↗](#)







Article views: 13



View Crossmark data [↗](#)



Prediction of pedestrian dynamics in complex architectures with artificial neural networks

Antoine Tordeux^a , Mohcine Chraïbi^b , Armin Seyfried^{b,c} , and Andreas Schadschneider^d 

^aSchool of Mechanical Engineering and Safety Engineering, University of Wuppertal, Wuppertal, Germany; ^bInstitute for Advanced Simulation, Forschungszentrum Jülich, Jülich, Germany; ^cSchool of Architecture and Civil Engineering, University of Wuppertal, Wuppertal, Germany; ^dInstitute for Theoretical Physics, University of Cologne, Cologne, Germany

ABSTRACT

Pedestrian behavior tends to depend on the type of facility. The flow at bottlenecks, for instance, can exceed the maximal rates observed in straight corridors. Consequently, accurate predictions of pedestrians movements in complex buildings including corridors, corners, bottlenecks, or intersections are difficult tasks for minimal models with a single setting of the parameters. Artificial neural networks are robust algorithms able to identify various types of patterns. In this paper, we will investigate their suitability for forecasting of pedestrian dynamics in complex architectures. Therefore, we develop, train, and test several artificial neural networks for predictions of pedestrian speeds in corridor and bottleneck experiments. The estimations are compared with those of a classical speed-based model. The results show that the neural networks can distinguish the two facilities and significantly improve the prediction of pedestrian speeds.

ARTICLE HISTORY

Received 31 August 2018
Revised 16 May 2019
Accepted 17 May 2019

KEYWORDS

Artificial neural network;
complex architecture;
prediction of
pedestrian dynamics

Introduction

Microscopic pedestrian models are frequently used in traffic engineering to predict crowd dynamics. Classical operational approaches are decision-based, velocity-based, or acceleration-based models (see Chraïbi, Tordeux, Schadschneider, and Seyfried, 2018; Schadschneider, Chraïbi, Seyfried, Tordeux, & Zhan, 2018; and references therein). Such models consider physical as well as social or psychological factors. They are defined by basic rules or generic functions depending locally on the environment. These models can be specified by a few parameters which generally have physical interpretations and allow to adjust the model.

Before applying simulations to make predictions, the model parameters have to be calibrated and the models have to be validated, experimentally or statistically by using real data. The validation can be carried out by checking whether the models are able to describe the dynamics accurately for configurations different from the ones used for the calibration (Treiber & Kesting, 2013). A robust model should provide realistic dynamics in different conditions (i.e. different geometries and initial or boundary conditions) for the same set of the parameters.

Nowadays, machine learning and data-based algorithms such as artificial neural networks (ANN) start to be used for prediction of pedestrian dynamics. Potential applications are forecasting of pedestrian movement in complex situations, including evacuations, or for motion planning of robots moving in a crowded environment (Chen, Everett, Liu, & How, 2017; Das, Parida, & Katiyar, 2015). The methodological approach with data-driven approaches consists in partitioning the dataset in training, testing, and predicting subsets (Kohavi, 1995). The predictions with machine learning approaches, having much more parameters, are generally more precise than those of physics-based models. Yet, training the algorithms generally requires a large amount of data and specific investigations to determine the necessary complexity of the network.

Bibliographical review

Microscopic pedestrian models used in traffic engineering for simulation and prediction are generally physics-based models based on few meaningful parameters. The main parameters are related to the

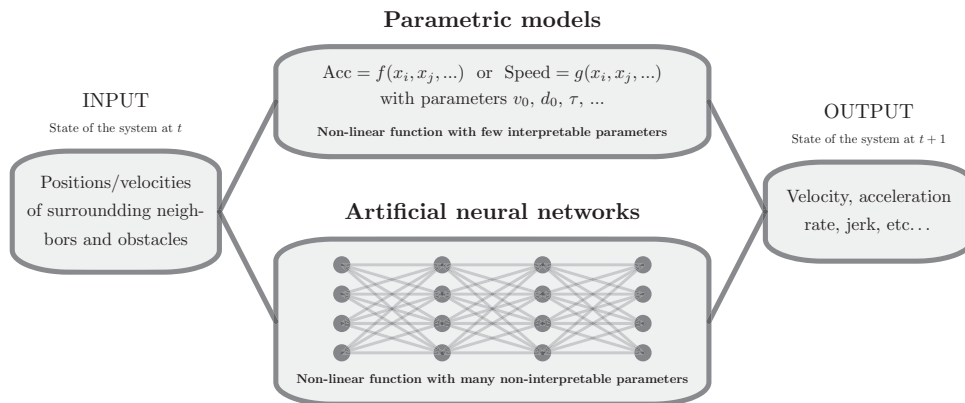


Figure 1. Minimalistic scheme for the distinction between parametric (physics-based) models and artificial neural networks for the prediction of pedestrian dynamics.

motion (for instance the desired speed or the following time gap) and the exclusion between the agents (e.g. agent size). Such parameters can be referred to the fundamental diagram (FD), a phenomenological relation between speed and surrounding distance spacing to the neighbors and obstacles (Predtechenskii & Milinskii, 1978). This relation can be explicitly used to model the speed of the pedestrian and is then related to the *optimal velocity*, a concept borrowed from traffic modeling (Bando, Hasebe, Nakayama, Shibata, & Sugiyama, 1995), see e.g. Lv, Song, Ma, and Fang (2013), Moussaïd et al. (2012), and Nakayama, Hasebe, and Sugiyama (2005). More generally, microscopic models incorporate parameters for the desired speed or agent size, however, the following time gap or other desired spacing are not explicitly defined (see e.g. Chraïbi, Seyfried, and Schadschneider, 2010; Guo, Wong, Huang, Zhang, and Lam, 2010; Helbing and Molnár, 1995). The interaction generally results as a sum of repulsion with the neighbors and attraction to a goal by the desired velocity. The fundamental diagram can be determined considering uni-directional flows and is generally used to validate the models (Chraïbi et al., 2015). See Chraïbi et al. (2018), Duives, Daamen, and Hoogendoorn (2013), and Schadschneider et al. (2018); for overviews on crowd motion models.

Despite their simplicity, microscopic parametric models can describe realistic pedestrian flows, as well as self-organization phenomena, such as lane formation or streaming alternation at bottlenecks in counter flows (Helbing, Buzna, Johansson, & Werner, 2005; Schadschneider et al., 2009). However, the prediction of pedestrian movement in complex spatial structures (e.g. buildings like sports arenas or stations) remains problematic. Observations show that pedestrians tend to adapt their behavior according to the facilities

(Daamen, 2004). For instance, the flow tends to locally increase at bottlenecks (Parisi & Patterson, 2017; Seyfried et al., 2009; Zhang & Seyfried, 2014), which points out to certain geometry-dependent characteristics of pedestrian dynamics. This dependency makes difficult the accurate description of transitions between different types of facilities (such as corridor, T-junction, crossing, or bottleneck) as well as from platforms to stairs with physics-based models based on a single set of the parameters.

Currently, artificial neural networks represent an alternative approach for the prediction of pedestrian dynamics in complex situations. The high plasticity of the networks allows, in theory, to describe any type of patterns. The approach is data-based. It has, in contrast to classical models, artificially a large number of parameters with no explicit physical meaning (see Figure 1). Indeed, neural networks are algorithms for prediction, they are not models. They have already proven their efficiency for motion planning in robotic or autonomous vehicles (see e.g. Jackel et al., 2007; Sadati and Taheri, 2002). Neural networks start to be used for predictions of pedestrian movements as well, notably in complex geometries (Das et al., 2015), for the motion planning of robots moving in a crowd (Chen et al., 2017), for generation of level-of-service maps in transport stations (Li, Khoshelham, Sarvi, & Haghani, 2019), for pedestrian detection of autonomous vehicles (Shladover, 2018; Zhang, Xin, & Wu, 2016), or for modeling of walker pose (Fragkiadaki, Levine, Felsen, & Malik, 2015). Simplest approaches are based on feed-forward neural networks (see Das et al., 2015; Ma, Lee, and Yuen, 2016) while the most sophisticated prediction algorithms lie in Long-Short Term Memory networks (Alahi et al., 2016; Li et al., 2019) or Deep Reinforcement Learning techniques (Chen et al., 2017).

Aim and organization of the paper

The aim of this work is to evaluate whether artificial neural networks can accurately describe pedestrian behavior in complex architectures, i.e. for combinations of different types of facilities. Several feed-forward neural networks based on pedestrian position, mean distance, and velocity are developed and compared with an elementary speed-based model based on three parameters. The data are taken from experiments at bottlenecks and in corridors with closed boundary conditions. The performances (i.e. the fundamental diagram) significantly differ according to the type of experiment and its spatial structure. One investigates the ability of neural networks to identify the specific patterns of each geometry and to improve the prediction in case of mixed facilities.

The paper is organized as follows. First, the speed-based model and the artificial neural networks are presented. The empirical data used for calibration, training and testing are described in the next section. The fitting of the networks is then detailed in while benchmark analyses for combinations of bottleneck and corridor experiments are presented in the following section. Some conclusions and perspectives of future works are proposed at the end of the article.

Speed model and neural networks

The objective is to predict the speed of pedestrians according to the positions and eventually the velocity of the K closest neighbors. We denote in the following (x, y) as the position of the considered agent, v as its speed and $((x_i, y_i), i = 1, \dots, K)$ and $((v_i, u_i), i = 1, \dots, K)$ as positions and velocities of the K closest neighbors.

Speed-based model

The first modeling approach is the parametric Weidmann fitting model for the fundamental diagram (Weidmann, 1994), for which the speed is a non-linear function of the mean spacing with three parameters:

$$W(\bar{s}_K, v_0, T, \ell) = v_0 \left(1 - e^{-\frac{\ell - \bar{s}_K}{v_0 T}} \right). \quad (1)$$

Here

$$\bar{s}_K = \frac{1}{K} \sum_i \sqrt{(x - x_i)^2 + (y - y_i)^2} \quad (2)$$

is the mean Euclidian spacing to the K closest neighbors. The time gap parameter T corresponds to the following time gap with the neighbors, v_0 is the speed

of pedestrians in a free situation while ℓ describes the physical size of a stopped pedestrian. In the following, the Weidmann's model Eq. (1) and its parameters are used as a benchmark.

Artificial neural networks

The second modeling approach for prediction of the pedestrian speed is feed-forward artificial neural networks with hidden layers h . The networks are algorithms providing through the hidden layers an output, here the pedestrian speed, as a function of given inputs. The hidden layers h consist of fully connected layers of elementary neurons with a sigmoid activation function. They describe the complexity of the algorithm. The inputs are the explanatory variables. Four networks with different inputs are developed and tested:

- In the first network, the inputs are the relative positions to the K closest neighbors ($2K$ inputs)

$$NN_1 = NN_1(x_i - x, y_i - y, 1 \leq i \leq K). \quad (3)$$

- In the second network, the speed is predicted as a function of the relative positions and relative velocities to the K closest neighbors ($4K$ inputs)

$$NN_2 = NN_2(x_i - x, y_i - y, v_i - v, u_i - u, 1 \leq i \leq K). \quad (4)$$

- The third network depends on the relative positions and also the mean distance spacing \bar{s}_K to the K closest neighbors ($2K + 1$ inputs)

$$NN_3 = NN_3(\bar{s}_K, (x_i - x, y_i - y, 1 \leq i \leq K)). \quad (5)$$

- Finally, the fourth network depends as well on relative positions, mean distance spacing and relative velocities to the K closest neighbors ($4K + 1$ inputs)

$$NN_4 = NN_4(\bar{s}_K, (x_i - x, y_i - y, v_i - v, u_i - u, 1 \leq i \leq K)). \quad (6)$$

The number of parameters in the network depends on the number of neighbors for the interaction K and on the number of artificial neurons in the hidden layers. They have in general no physical interpretation. We set the parameter K up to 10 in the following. Smaller K tends to increase the variability of the data while larger K provides smoother results close to mean ones. Experimentally, we observe that setting K up to 10 is a reasonable compromise.

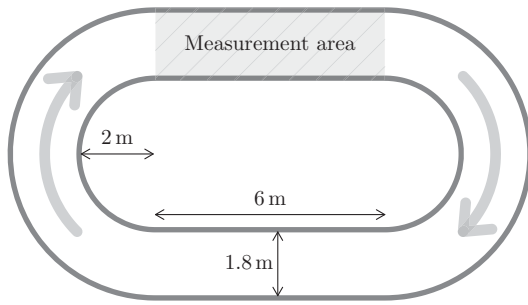


Figure 2. Scheme of the corridor (C) experiment with pedestrians walking on a closed geometry. Several experiments are carried out for different density levels (ranging from approximately 0.25 to 2 ped/m²).

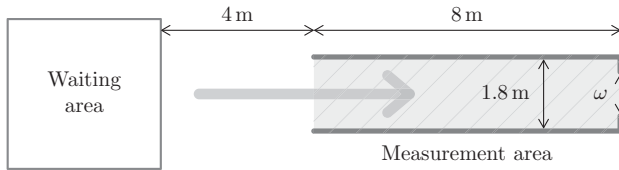


Figure 3. Scheme of the bottleneck (B) experiment with pedestrians walking on a corridor and a bottleneck. Four experiments are carried out for different bottleneck widths $\omega = 0.70, 0.95, 1.20$, and 1.80 m. 150 walkers participated in each experiment.

Empirical data

Two datasets of pedestrian trajectories obtained from experiments in laboratory conditions are used to train and test the speed model and the artificial neural networks and for comparison with the predictions. One experiment was realized in a corridor geometry while the other was carried out in a bottleneck. See the Figures 2 and 3 for the schemes of the experiments (both schemes in Figures 2 and 3 have the same spatial scale). The experiments were performed in 2009 in Düsseldorf, Germany, as part of the research project Hermes (Holl, Schadschneider, & Seyfried, 2014). The instructions given to the participants were to walk naturally without any rush or haste. The trajectories of all test persons are determined by semi-automatic video analysis (video frame rate: 16 frame/s). The positions of the pedestrians and the positions of the closest neighbors are measured. The speeds are obtained by differentiating the positions over one second. Only one measurement each 5 s is used to deal with pseudo-independent observations. Each sample contains around $n = 2100$ observations. The data and their description are available on the internet (see Tordeux, Chraïbi, Seyfried, and Schadschneider, 2017). They are part of the online database of pedestrian experiments Forschungszentrum Jülich (2018c).

Corridor experiment

The first dataset, denoted by C for “corridor experiment,” comes from an experiment done in a corridor of length 30 m and width 1.8 m with periodic boundary condition with participants walking in the same direction (see Forschungszentrum Jülich, 2018b; Tordeux et al., 2017; Zhang, 2012; Forschungszentrum Jülich, 2018d, p. 20, for further details regarding the setting-up of the corridor experiment). The trajectories are measured on a straight section of length 6 m (see Figure 2). Eight experiments are carried out with 15, 30, 60, 85, 95, 110, 140, and 230 participants (i.e. for density levels ranging from approximately 0.25 to 2 ped/m²).

Bottleneck experiment

The second dataset denoted B, is an experiment on bottleneck flow. The width of the corridor in front of the bottleneck is 1.8 m while the width of the bottleneck varies from 0.70, 0.95, 1.20 to 1.80 m in four distinct experiments. A total of 150 participants are involved for each experiment (see Forschungszentrum Jülich, 2018a; Liao et al., 2014; Tordeux et al., 2017; Zhang, 2012; Forschungszentrum Jülich, 2018d, p. 24, for further details on the bottleneck experiment).

Data analysis

The two data sets for the corridor and the bottleneck experiments describe two slightly different interaction behaviors (see Figure 4). The speed for a given mean spacing tends to be higher in the bottleneck than in the corridor when the system is congested. This suggests that pedestrians accept to walk temporally at the same mean spacing faster and closer in a bottleneck than in a corridor. Indeed, estimations by least squares of the time gap T and the desired speed v_0 for the Weidmann’s model Eq. (1) differ according to the experiment (resp. around 0.85 s and 1.50 m/s for the corridor, and 0.49 s and 1.64 m/s for the bottleneck, see Table 1). The pedestrian size ℓ remains approximately constant. Note that the mean spacing is around 10% smaller in the corridor than in the bottleneck (resp. 1.03 and 1.14 m). However, the mean speed is more than two times bigger in the bottleneck (0.35 and 0.72 m/s, see Table 1). The distribution of the mean spacing to the 10 closest neighbors is more concentrated for the bottleneck than for the corridor (see Figure 5). The distributions of the speed show a double-peak structure, especially for the bottleneck.

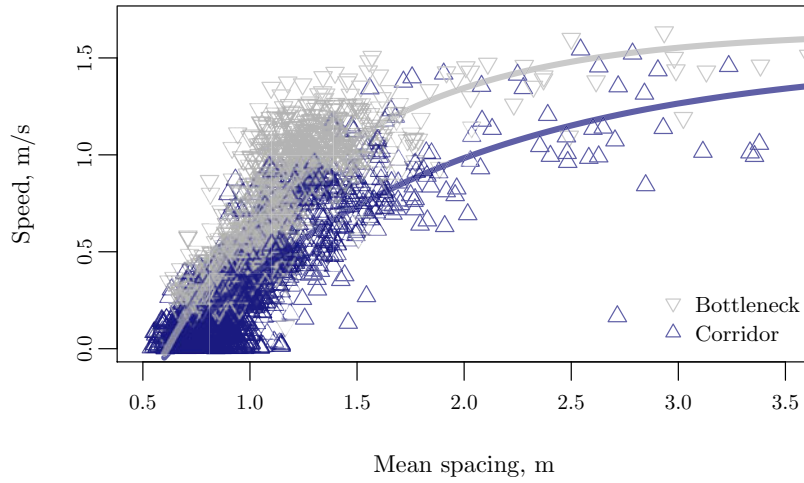


Figure 4. Pedestrian speeds as function of the mean spacing with the 10 closest neighbors for the corridor and bottleneck experiments and respective least squares fitting for the Weidmann's model. Two distinct relationships can be identified.

Table 1. Mean value and standard deviation of the speed and the spacing and least squares estimation of the time gap T , the pedestrian size ℓ and the desired speed v_0 parameters of the Weidmann's model Eq. (1) for the corridor and bottleneck experiments.

Experiment	Parameter			Mean value	
	ℓ (m)	T (s)	V_0 (m/s)	Spacing (m)	Speed (m/s)
Bottleneck	0.61	0.49	1.64	1.14 ± 0.37	0.72 ± 0.34
Corridor	0.64	0.85	1.50	1.03 ± 0.40	0.35 ± 0.33

Fitting the neural networks

Mean square error

The neural networks are fitted through training and testing phases (cross-validation). Bootstrapping is done to evaluate the precision of estimation (Kohavi, 1995; Mooney & Duval, 1993). The training is performed using randomly half of the data while the networks are tested on the remaining observations. The training is carried out with the back-propagation method (Rumelhart, Hinton, & Williams, 1986) on the normalized dataset, by minimizing the mean square error (MSE)

$$\text{MSE} = \frac{1}{n} \sum_{i=1}^n (v_i - \tilde{v}_i)^2. \quad (7)$$

Here v_i are the observed speeds, \tilde{v}_i the predicted speeds and n is the number of observations. 50 bootstrap sub-samples are carried out for each estimation. The computation is done with R (R Core Team, 2014) and the package neuralnet (Fritsch, Guenther, & Suling, 2012).

Setting the network complexity

Eight different hidden layers h are tested for the neural networks. The simplest network is composed

of a single neuron while the more complex one contains two layer of respectively 10 and 4 neurones. If a and b are the number of neurons of the first and second layers, on denote the hidden layers $h = (a, b)$ (resp. $h = (a)$ if $b = 0$). The tested hidden layers h are (1), (2), (3), (4,2), (5,2), (5,3), (6,3), and (10,4).

The training and testing errors for these layers on the full dataset combining the corridor and bottleneck experiment datasets (denoted C + B/C + B in the following) are presented in Figure 6. As expected, the training error tends to monotonically decrease as the complexity of the network increases, while the testing error shows a minimum before overfitting. Such systematic U-shape allows determining the optimal structure for the neural networks. Yet, the minimum depends on the input provided to the networks. Roughly speaking, it is reached for the single hidden layer $h = (3)$ with three nodes for networks NN_3 and NN_4 based on the mean distance spacing and the relative positions and velocities, while it is reached for $h = (5,3)$ for the networks NN_1 and NN_2 solely based on the relative positions and velocities. The information brought by the mean spacing allows to reduce the complexity of the network structures.

Predictions for the speed

Predictions for combinations of experiments

The four neural networks NN_1 , NN_2 , NN_3 , and NN_4 (see Eqs. (3)–(6)) are trained and tested for combinations of the corridor (C) and bottleneck (B) experiments. The speed model by Weidmann Eq. (1) is calibrated by least squares on the same datasets. It will be used as a benchmark in the following. The objective is to evaluate whether the networks are able

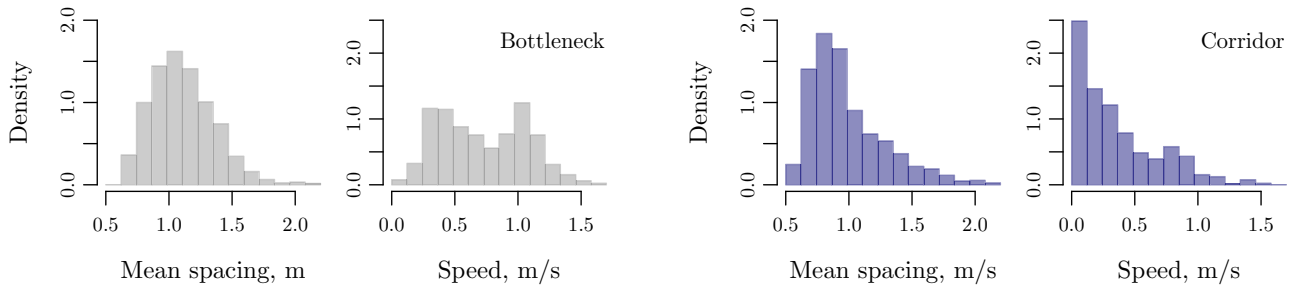


Figure 5. Histograms for the mean spacing to the 10 closest neighbors and the speed for the bottleneck and corridor experiments.

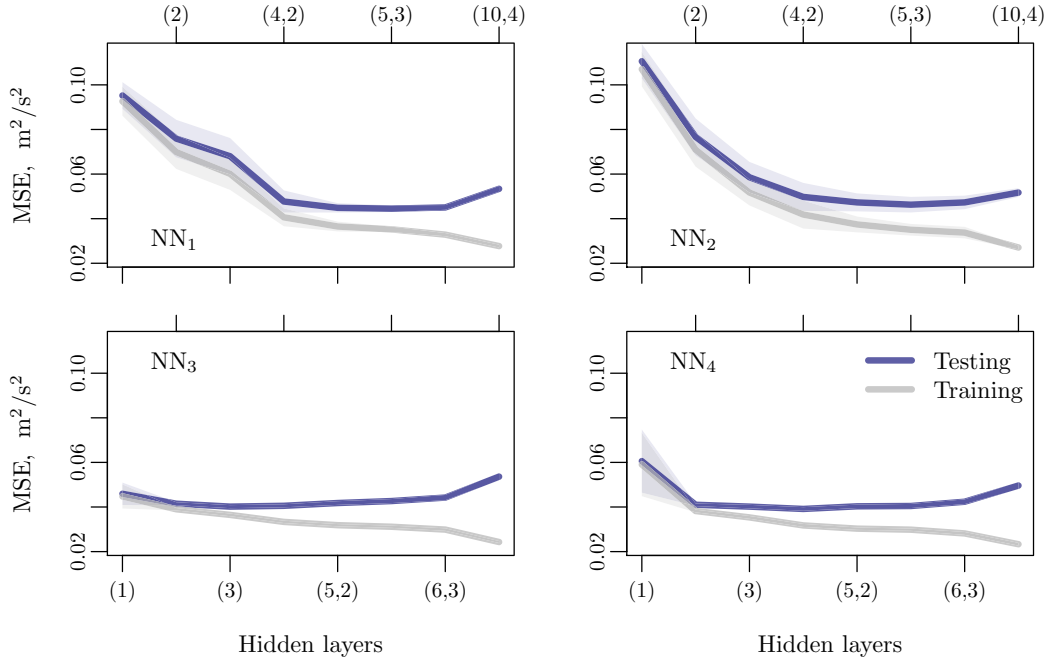


Figure 6. Training and testing errors according to different hidden layers in the networks. The curves correspond to the average of 50-bootstrap estimates while the bands describe 0.99-confidence intervals. The training errors systematically decrease as network complexity increases while the testing errors admit minimums.

to identify and predict the pattern of each experiment. In the following, the first argument X in the notation ' X/Y ' corresponds to the dataset used for the training phase, while the second argument Y corresponds to the dataset used for the testing phase. For instance, B/C corresponds to the prediction for the corridor experiments with a network trained on the bottleneck experiment. The testing is performed using half of the data, the training being carried out on the remaining observations.

Seven combinations of the corridor (C) and bottleneck (B) experiments are analysed:

- B/B and C/C . Here a single dataset is used for both training and testing.
- B/C and C/B . Such cases are used to test the ability for prediction in new situations.

- $C + B/B$, $C + B/C$, and $C + B/C + B$ are used to test prediction in heterogeneous situations.

These combinations of training and testing sets are carried out for hidden layers $h = (1), (2), (3), (4,2), (5,2), (5,3), (6,3)$, and $(10,4)$ and in the bootstrap framework with 50 independent subsamples. The best network complexities are relatively high for networks NN_1 and NN_2 depending solely on relative positions and velocities (i.e. hidden layer $h = (5,2), (5,3)$, or $(6,3)$, see Figures 7 and 8) for any combination of experiments. Networks NN_3 and NN_4 depending additionally on the mean spacing require less complexity (i.e. $h = (2), (3)$, or $(4,2)$, see Figures 9 and 10). This is in agreement with the results presented in Figure 6. The precision of the estimations is relatively low for both networks NN_1 and NN_2 . This is due to a lack of

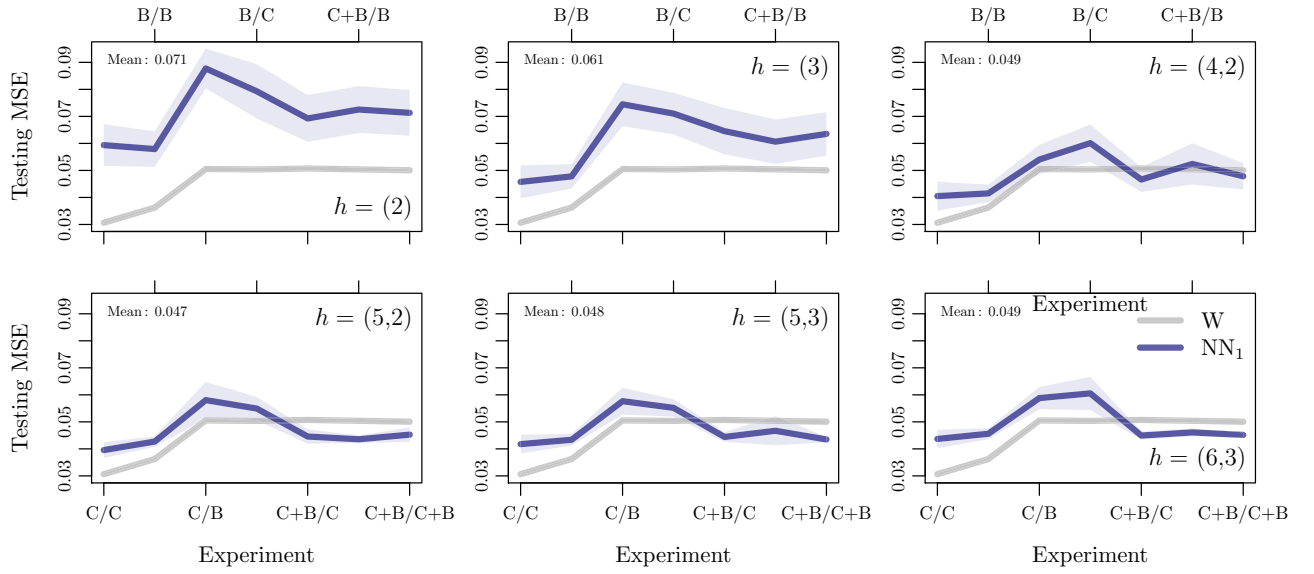


Figure 7. Testing error for the Weidmann's model Eq. (1) and the neural network NN_1 based on the relative positions (see Eq. (3)) for the seven combinations of corridor (C) and bottleneck (B) experiments. The curves are the average of 50-bootstrap estimates while the bands are 0.99-confidence intervals.

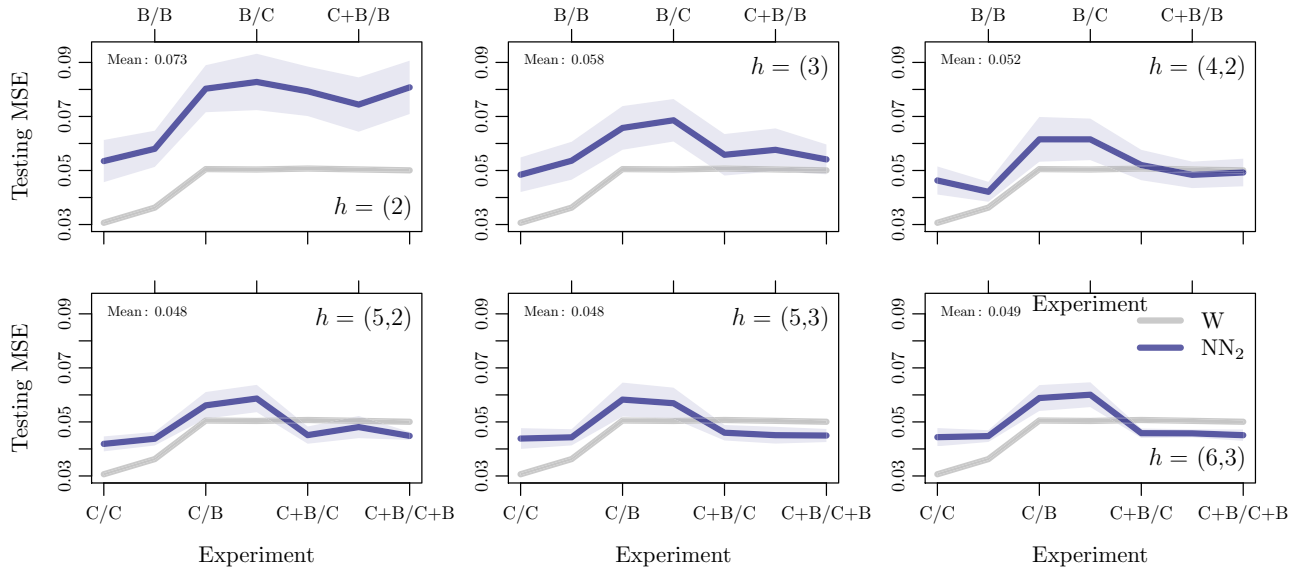


Figure 8. Testing error for the Weidmann's model Eq. (1) and the neural network NN_2 based on the relative positions and relative velocities (see Eq. (4)) for the seven combinations of corridor (C) and bottleneck (B) experiments. The curves are the average of 50-bootstrap estimates while the bands are 0.99-confidence intervals.

data. Adding the mean spacing in the input, even if resulting from the relative positions, allows to reduce the complexity of the network and so the amount of data necessary for the training, and to improve the predictions. A summary of the results is given in Table 2.

Optimal neural structure

By optimizing with respect to the number of hidden layers and neurons, we set in the following the two hidden layers structure $h = (5, 3)$ for the networks NN_1 and NN_2 and the one hidden layer structure $h =$

(3) for NN_3 and NN_4 . The testing error for each of these four networks is compared with the testing error of the Weidmann's model in Figure 11. The predictions for the networks NN_1 and NN_2 solely based on relative positions and velocities are, due to a lack of data, worth than those of the Weidmann's model for any combination of single experiments (i.e. scenarios C/C, B/B, C/B, and B/C). The networks NN_3 and NN_4 based on mean spacing are equivalent to the Weidmann's model for the corridor experiment C/C, and better for the bottleneck B/B (around 10%) or when the networks deal with unobserved situations,

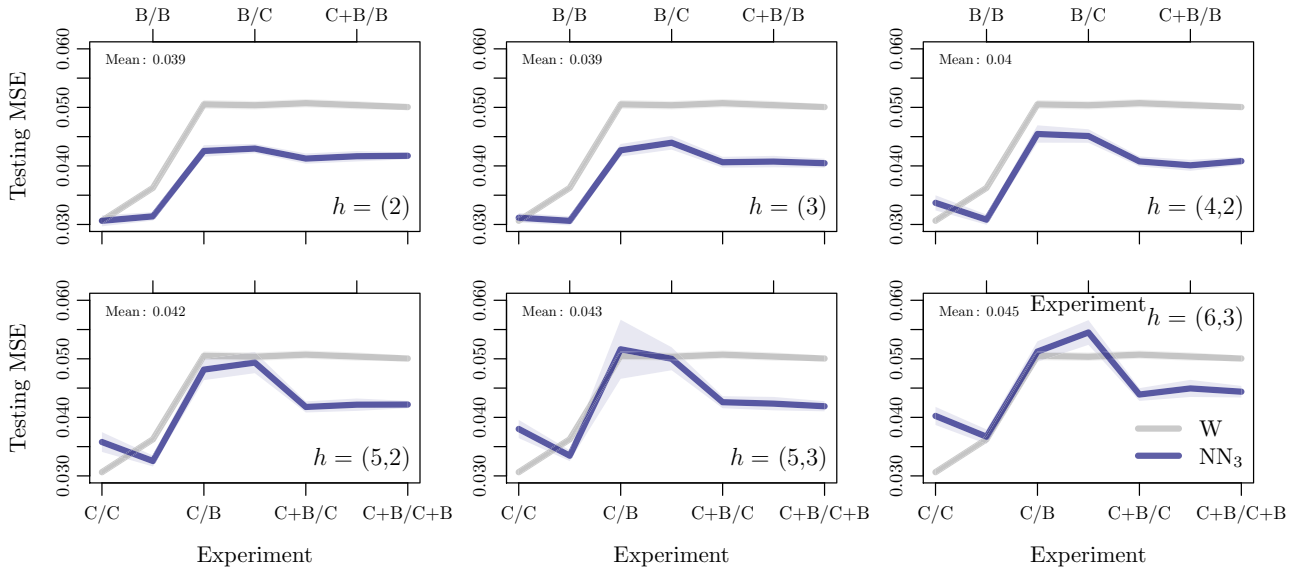


Figure 9. Testing error for the Weidmann's model Eq. (1) and the neural network NN_3 based on the relative positions and mean spacing (see Eq. (5)) for the seven combinations of corridor (C) and bottleneck (B) experiments. The curves are the average of 50-bootstrap estimates while the bands are 0.99-confidence intervals.

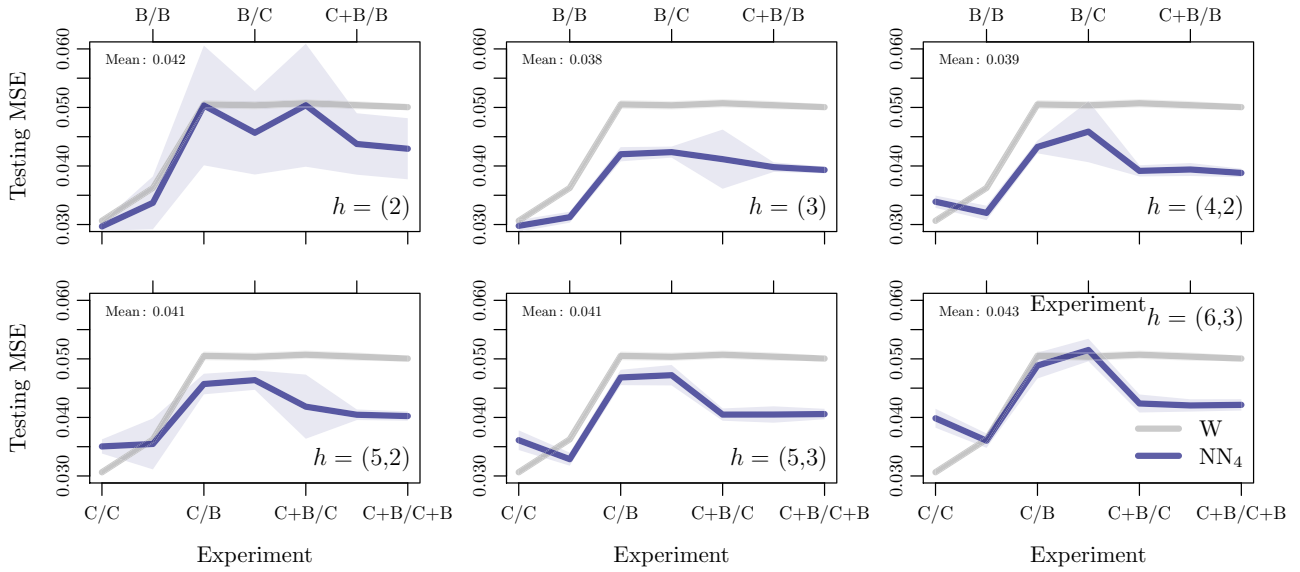


Figure 10. Testing error for the Weidmann's model Eq. (1) and the neural network NN_4 based on the relative positions, mean spacing and relative velocity (see Eq. (6)) for the seven combinations of corridor (C) and bottleneck (B) experiments. The curves are the average of 50-bootstrap estimates while the bands are the 0.99-confidence intervals.

i.e. for C/B and B/C (around 15%). Such a last result attests for the robustness of the networks NN_3 and NN_4 for prediction in case of new scenarios.

All the networks improve the prediction in case of mixed dataset, i.e. the scenarios C/C + B, B/C + B, and C + B/C + B. The improvement in terms of MSE are around 10% for the networks NN_1 and NN_2 and around 20% for the networks NN_3 and NN_4 based on the mean spacing. The orders of improvement are similar to the ones obtained in Alahi et al. (2016) with the social LSTM neural network and the social force pedestrian model

(Helbing & Molnár, 1995) or in Das et al. (2015) for traffic flow with a feed-forward ANN with four layers and 20 neurons and the classical Greenshield (Greenshields, 1935) and Greenberg (Greenberg, 1959) models.

Note that the adding of the velocity in the inputs of the networks (i.e. networks NN_2 and NN_4) does not clearly improve the predictions. This may be due to the fact that the experiments involve only unidirectional pedestrian flows. The relative velocity could bring better predictions in case of multi-directional flows, for instance for counter- or crossing flows.

Quality of the fit

Since we deal with pseudo-independent observations, the residuals

$$z_i = v_i - \tilde{v}_i, \quad i = 1, \dots, n \quad (8)$$

v_i and \tilde{v}_i being respectively the observed and predicted speeds and n the number of observations, can be considered independent. If we moreover suppose that the

Table 2. Mean value and standard deviation of the testing MSE for the neural networks NN_1 , NN_2 , NN_3 , and NN_4 (see Eqs. (3)–(6)) according to the network complexity h (see Figures 7–10).

Network		Hidden layers h							
		(1)	(2)	(3)	(4,2)	(5,2)	(5,3)	(6,3)	(10,4)
NN_1	Mean	0.091	0.071	0.061	0.049	0.047	0.048	0.049	0.059
	Dev.	0.013	0.023	0.020	0.015	0.009	0.009	0.008	0.007
NN_2	Mean	0.101	0.073	0.058	0.052	0.048	0.048	0.049	0.060
	Dev.	0.017	0.025	0.020	0.016	0.009	0.011	0.008	0.008
NN_3	Mean	0.042	0.039	0.039	0.040	0.042	0.043	0.045	0.053
	Dev.	0.008	0.002	0.003	0.003	0.003	0.005	0.004	0.006
NN_4	Mean	0.053	0.042	0.038	0.039	0.041	0.041	0.043	0.053
	Dev.	0.031	0.017	0.004	0.004	0.006	0.004	0.004	0.006

The mean MSE and standard deviation for the speed-based model Eq. (1) are 0.046 and 0.002. The values minimizing the MSE and its standard deviation are indicated in bold.

residuals are normally distributed (see Figure 12), the logarithm of the maximal likelihood for the least squares estimates is

$$\ell_n = -\frac{n}{2}(1 + \ln(2\pi)) - \frac{n}{2} \ln(\text{MSE}). \quad (9)$$

The Akaike Information Criterion (AIC) is then (see e.g. Burnham & Anderson, 2002)

$$\text{AIC} = 2k - 2\ell_n = 2k + n \ln(\text{MSE}) + n(1 + \ln(2\pi)), \quad (10)$$

with k the number of parameters of the prediction algorithm. We have $k_W = 3$ for the parametric Weidmann's model. Each neuron of the neural networks contains $I + 1$ parameters, I being the number of inputs in the algorithms. The number of inputs of the networks are $I_1 = 2K$, $I_2 = 4K$, $I_3 = 2K + 1$, and $I_4 = 4K + 1$, K being the number of neighbors for the interaction, while their optimal numbers of neurons are 9, 9, 4, and 4 (see Figure 11). Since $K = 10$, the number of parameters of the neural networks NN_1 , NN_2 , NN_3 , and NN_4 are respectively $k_1 = 189$, $k_2 = 369$, $k_3 = 88$, and $k_4 = 168$.

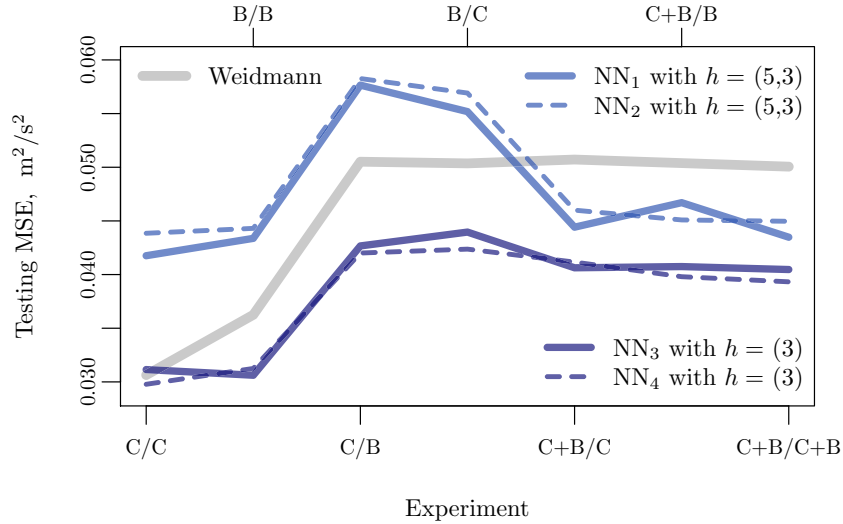


Figure 11. Testing error for the optimal complexity for each of the four neural networks NN_1 , NN_2 , NN_3 , and NN_4 (see Eqs. (3)–(6)) and the error of the Weidmann's model (see Eq. (1)).

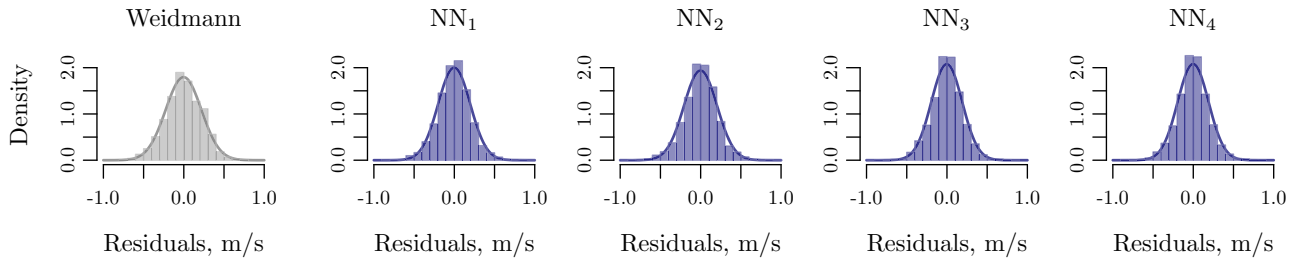


Figure 12. Histograms of the speed residuals $z_i = v_i - \tilde{v}_i$, with v_i the observed and \tilde{v}_i the predicted speeds, and the empirical normal distribution (continuous curves) for the Weidmann's model (left panel) and the neural networks NN_1 , NN_2 , NN_3 , and NN_4 for the heterogeneous scenario $C + B/C + B$.

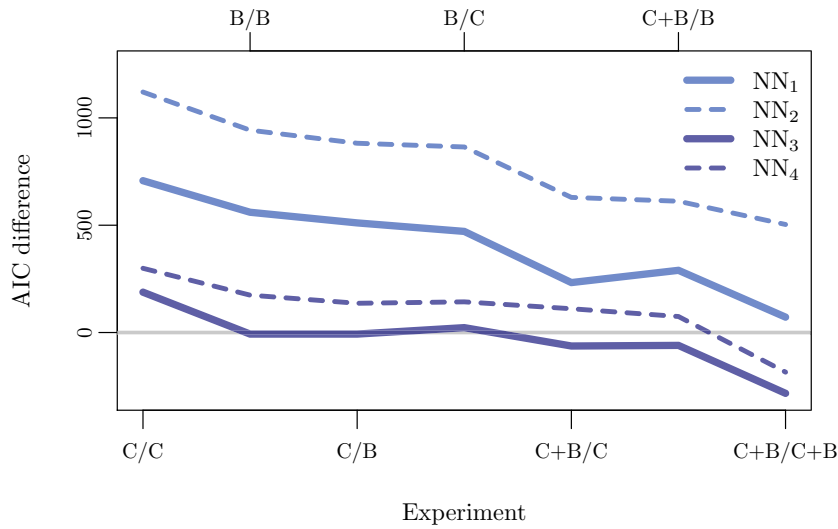


Figure 13. AIC differences of the neural networks NN_1 , NN_2 , NN_3 , and NN_4 (see Eqs. (3)–(6)) to the AIC of the Weidmann's model Eq. (1). The networks better describe the data than the Weidmann's model relatively to the parameter number when the AIC difference is negative.

Table 3. Mean MSE and AIC over all the scenarios for the predictions given by the Weidmann's model Eq. (1) and by the four neural networks NN_i , $i = 1, \dots, 4$, Eqs. (3)–(6).

	Weidmann's model	Network			
		NN_1	NN_2	NN_3	NN_4
Mean MSE	0.046	0.048	0.048	0.039	0.038
Mean AIC	−304	102	489	−334	−196

The values minimizing the mean MSE and mean AIC are indicated in bold.

The AIC differences of the neural networks to the AIC of the Weidmann's model are presented in Figure 13. The networks better describe the data than the Weidmann speed model relatively to the parameter number when the AIC difference is negative. Even if the number of parameters is relatively important for the neural networks, we observe that the network NN_3 based on the relative positives and mean distance spacing present a better AIC than the Weidmann's model, especially for heterogeneous walking situations (i.e. for the scenarios C/C + B, B/C + B, and C + B/C + B). In simple scenarios (i.e. scenarios C/C and B/B), the Weidmann's model systematically better performs. The mean MSE and AIC over all the scenarios are presented in Table 3. The neural network NN_4 presents the lower mean square error while the network NN_3 minimizes the mean Akaike information criterion.

Predictions for the heterogeneous scenario

Some examples of predictions obtained with the neural networks Eqs. (3)–(6) for the heterogeneous scenario C + B/C + B combining both corridor and bottleneck experiments are presented in Figure 14. The increase of the performances observed in the

bottleneck experiment for the real data is, even partially, predicted. Indeed, the neural networks seem able to identify the two experiments and their specific patterns and to predict the speed accordingly. Estimations for the three parameters of the Weidmann's model Eq. (1) for corridor and bottleneck experiments are separately provided in the Table 4. The estimations for the parameter ℓ describing the agent size does not clearly depend on the experiment. However, the time gap T significantly decreases for the bottleneck experiment (from roughly 0.7 s for the corridor and 0.5 s for the bottleneck; the difference is more accentuated again for the real data, resp. 0.9 and 0.5 s, see Table 1). The desired speed is also slightly higher for the bottleneck, even if underestimated (around 1.55 for 1.4 m/s in the corridor; resp. 1.64 and 1.5 m/s for the real data). Furthermore, the speed tends to be higher in the bottleneck than in the corridor (resp. 0.64 and 0.43 m/s; 0.72 and 0.35 m/s for the real data), and the speed distributions tend to describe a double-peak structure (see Figure 15). Further results present similar trends when repeating the prediction by bootstrap and looking to the averaged estimates.

Conclusion

In this article, artificial neural networks are developed for the prediction of pedestrian dynamics in two different walking situations, namely a corridor and a bottleneck. The data-driven approach is able to distinguish pedestrian performances according to the facility from the relative positions of the $K = 10$ closest neighbors. Indeed, the predictions for mixed data combining both the corridor and bottleneck experiments are

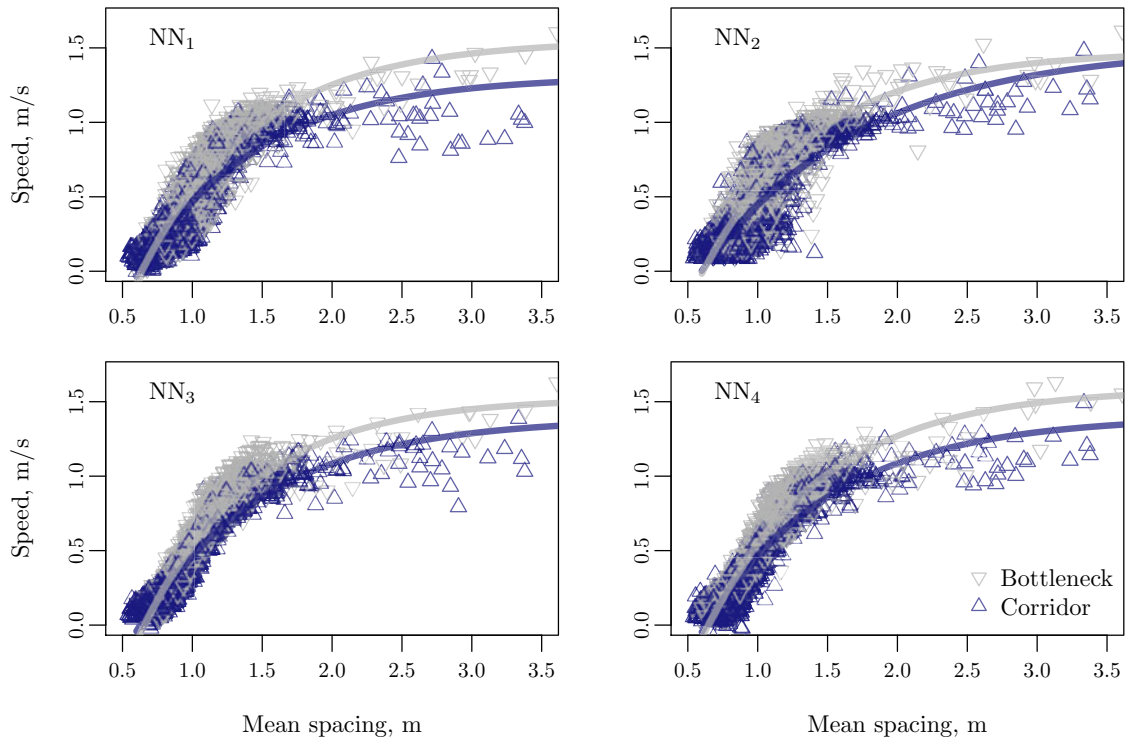


Figure 14. Examples of predictions by the neural networks Eqs. (3)–(6) for the heterogeneous scenario C + B/C + B. As observed in the real data, the speed for a given mean spacing tends to be in average in the bottleneck higher than in the corridor.

Table 4. Estimations for the pedestrian size ℓ , the time gap T and the desired speed v_0 parameters for the predictions given by the Weidmann's model Eq. (1) and by the four neural networks NN_i , $i = 1, \dots, 4$, Eqs. (3)–(6), according to the corridor and bottleneck experiments (see Figure 12).

Exp.		Weidmann's model		Network							
		C	B	NN ₁ C	B	NN ₂ C	B	NN ₃ C	B	NN ₄ C	B
ℓ	(m)	0.64		0.62	0.64	0.60	0.61	0.63	0.66	0.63	0.65
T	(s)	0.57		0.65	0.53	0.76	0.55	0.65	0.51	0.65	0.53
v_0	(m/s)	1.46		1.31	1.55	1.51	1.48	1.39	1.53	1.40	1.59
Mean speed	(m/s)	0.46	0.60	0.43	0.64	0.42	0.65	0.43	0.64	0.43	0.64

The closest values to the estimates for the real data are indicated in bold (see Table 1).

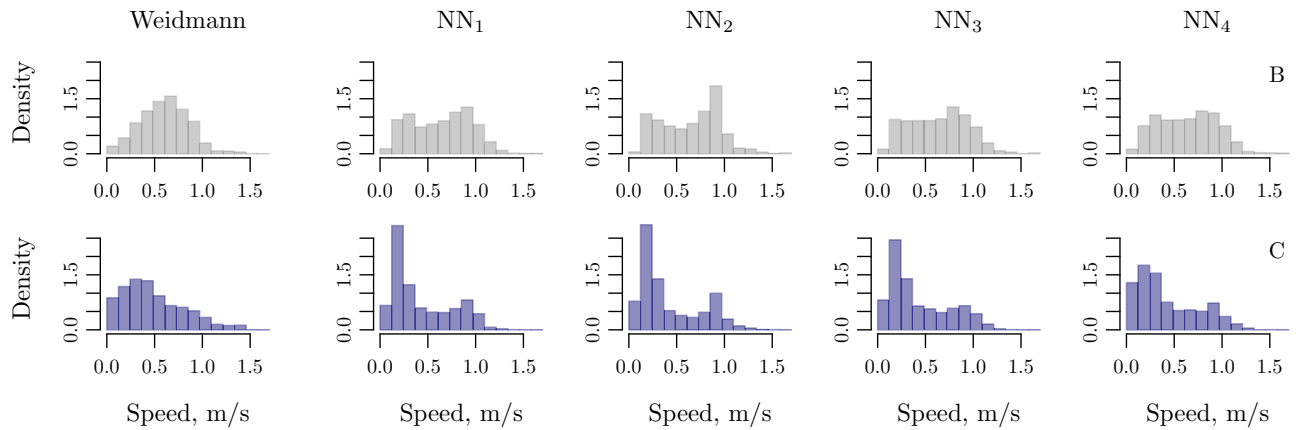


Figure 15. Histograms of the speed predictions of the heterogeneous scenario C + B/C + B for the Weidmann's model Eq. (1) and the networks NN_1 , NN_2 , NN_3 , and NN_4 (see Eqs. (3)–(6)). The estimates for the bottleneck experiment are presented in the top panels while the corridor experiment is described in the bottom panels. The real data are presented in Figure 5.

improved by a factor up to 20% compared with an elementary speed model based on three parameters. Furthermore, prediction in case of new situations, i.e. prediction of the speed in a bottleneck for networks trained on the corridor or inversely, are also significantly improved (by a factor up to 15%), attesting for the robustness of the networks.

Adding the mean spacing in the input of the networks, even if resulting from the relative positions, significantly increases the quality of the prediction. It also allows to reduce the complexity of the algorithm, and therefore the amount of data necessary for training. This is particularly useful when dealing with relatively small datasets. In contrast, adding the relative velocities with the neighbors does not lead to significant improvement. Yet, the tested experiments only deal with unidirectional flows. The velocity difference may improve the networks for multi-directional pedestrian flows, e.g. for crossing or counter-flows. This remains to be tested.

The results are first steps suggesting that neural networks could be suitable and robust algorithms for the prediction of pedestrian dynamics in complex architectures including different types of facilities. Data collection, methods for training and setting of the network complexity have to be developed and experimentally tested. The simulation of the networks remains to be carried out over full trajectories and compared with the performances obtained with other existing microscopic models, and notably anisotropic models and multi-agent systems. The number of neighbors for the interaction K is fixed in the analysis, up to 10. More robust networks should have a variable number of inputs and neighbors for the interaction, depending notably on the density level of the crowd and on the perception capacity of the pedestrians. This will be the topics of future works.

Disclosure statement

No potential conflict of interest was reported by the authors.

Funding

This work was supported by the German Science Foundation (DFG) under Grants SCHA 636/9-1 and SE 1789/4-1; Visiting Professor International project at the University of Science and Technology of China under Grant 2017B VR40.

ORCID

Antoine Tordeux  <http://orcid.org/0000-0001-5077-0327>
Mohcine Chraïbi  <http://orcid.org/0000-0002-0999-6807>

Armin Seyfried  <http://orcid.org/0000-0001-8888-0978>
Andreas Schadschneider  <http://orcid.org/0000-0002-2054-7973>

References

- Alahi, A., Goel, K., Ramanathan, V., Robicquet, A., Fei-Fei, L., & Savarese, S. (2016). *Social LSTM: Human trajectory prediction in crowded spaces*. Paper presented at the IEEE ICCV Conference, Las Vegas, NV, USA (pp. 961–971).
- Bando, M., Hasebe, K., Nakayama, A., Shibata, A., & Sugiyama, Y. (1995). Dynamical model of traffic congestion and numerical simulation. *Physical Review E*, 51(2), 1035–1042.
- Burnham, K., & Anderson, D. (2002). *Model selection and multimodel inference*. New York, NY: Springer.
- Chen, Y., Everett, M., Liu, M., & How, J. P. (2017). *Socially aware motion planning with deep reinforcement learning*. Paper presented at the IEEE IROS Conference (pp. 1343–1350), Vancouver, BC, Canada.
- Chraïbi, M., Ezaki, T., Tordeux, A., Nishinari, K., Schadschneider, A., & Seyfried, A. (2015). Jamming transitions in force-based models for pedestrian dynamics. *Physical Review E*, 92, 042809.
- Chraïbi, M., Seyfried, A., & Schadschneider, A. (2010). Generalized centrifugal-force model for pedestrian dynamics. *Physical Review E*, 82(4), 046111.
- Chraïbi, M., Tordeux, A., Schadschneider, A., & Seyfried, A. (2018). Modelling of pedestrian and evacuation dynamics (2nd ed.). In R. A. Meyers (Ed.), *Encyclopedia of complexity and systems science* (pp. 1–22). Berlin: Springer.
- Daamen, W. (2004). *Modelling passenger flows in public transport facilities* (Dissertation), TU Delft, Delft, The Netherlands.
- Das, P., Parida, M., & Katiyar, V. K. (2015). Analysis of interrelationship between pedestrian flow parameters using artificial neural network. *Journal of Modern Transportation*, 23(4), 298–309. doi:10.1007/s40534-015-0088-9
- Duives, D. C., Daamen, W., & Hoogendoorn, S. P. (2013). State-of-the-art crowd motion simulation models. *Transportation Research Part C: Emerging Technologies*, 37, 193–209. doi:10.1016/j.trc.2013.02.005
- Forschungszentrum Jülich. (2018a). Bottleneck experiment. Retrieved from <http://ped.fz-juelich.de/da/2009unidirClosed>
- Forschungszentrum Jülich. (2018b). Corridor experiment. Retrieved from <http://ped.fz-juelich.de/da/2009bottleneck>
- Forschungszentrum Jülich. (2018c). Dataset of experimental pedestrian trajectories. Retrieved from <http://ped.fz-juelich.de/database>
- Forschungszentrum Jülich. (2018d). Dokumentation von Versuchen zur Personenstromdynamik – Projekt “HERMES”. Retrieved from http://ped.fz-juelich.de/experiments/2009.05.12_Duesseldorf_Messe_Hermes/docu/VersuchsdokumentationHERMES.pdf
- Fragkiadaki, K., Levine, S., Felsen, P., & Malik, J. (2015). *Recurrent network models for human dynamics*. Paper presented at the IEEE ICCV Conference (pp. 4346–4354), Santiago, Chile.
- Fritsch, S., Guenther, F., & Suling, M. (2012). Neuralnet: Training of neural networks [Computer software

- manual]. Retrieved from <http://CRAN.R-project.org/package=neuralnet>
- Greenberg, H. (1959). An analysis of traffic flow. *Operations Research*, 7(1), 79–85. doi:10.1287/opre.7.1.79
- Greenshields, B. (1935). A study of traffic capacity. Paper presented at the Highway Research Board Proceedings (Vol. 14, pp. 448–477), Washington, DC.
- Guo, R., Wong, S., Huang, H., Zhang, P., & Lam, W. (2010). A microscopic pedestrian-simulation model and its application to intersecting flows. *Physica A*, 389(3), 515–526. doi:10.1016/j.physa.2009.10.008
- Helbing, D., Buzna, L., Johansson, A., & Werner, T. (2005). Self-organized pedestrian crowd dynamics: Experiments, simulations, and design solutions. *Transportation Science*, 39(1), 1–24. doi:10.1287/trsc.1040.0108
- Helbing, D., & Molnár, P. (1995). Social force model for pedestrian dynamics. *Physical Review E*, 51(5), 4282–4286.
- Holl, S., Schadschneider, A., & Seyfried, A. (2014). Hermes: An evacuation assistant for large arenas. In U. Weidmann, U. Kirsch, & M. Schreckenberg (Eds.), *Pedestrian and evacuation dynamics 2012* (pp. 345–349). Cham: Springer International Publishing.
- Jackel, L., Hackett, D., Krotkov, E., Perschbacher, M., Pippine, J., & Sullivan, C. (2007). How DARPA structures its robotics programs to improve locomotion and navigation. *Communications of the ACM*, 50(11), 55–59. doi:10.1145/1297797.1297823
- Kohavi, R. (1995). A study of cross-validation and bootstrap for accuracy estimation and model selection. In C. S. Mellish (Ed.), *Proceedings of the 14th international joint conference on artificial intelligence* (Vol. 2, pp. 1137–1143). San Francisco, CA: Morgan Kaufmann Publishers Inc.
- Li, Y., Khoshelham, K., Sarvi, M., & Haghani, M. (2019). Direct generation of level of service maps from images using convolutional and long short-term memory networks. *Journal of Intelligent Transportation Systems*, 23(3), 300–308. doi:10.1080/15472450.2018.1563865
- Liao, W., Seyfried, A., Zhang, J., Boltes, M., Zheng, X., & Zhao, Y. (2014). Experimental study on pedestrian flow through wide bottleneck. *Transportation Research Procedia*, 2, 26–33. doi:10.1016/j.trpro.2014.09.005
- Lv, W., Song, W.-g., Ma, J., & Fang, Z.-m. (2013). A two-dimensional optimal velocity model for unidirectional pedestrian flow based on pedestrian's visual hindrance field. *IEEE Transactions on Intelligent Transportation Systems*, 14(4), 1753–1763. doi:10.1109/TITS.2013.2266340
- Ma, Y., Lee, E. W. M., & Yuen, R. K. K. (2016). An artificial intelligence-based approach for simulating pedestrian movement. *IEEE Transactions on Intelligent Transportation Systems*, 17(11), 3159–3170. doi:10.1109/TITS.2016.2542843
- Mooney, C., & Duval, R. (1993). *Bootstrapping: A nonparametric approach to statistical inference*. Thousand Oaks, CA: SAGE Publications.
- Moussaïd, M., Guillot, E., Moreau, M., Fehrenbach, J., Chabiron, O., Lemerrier, S., ... Theraulaz, G. (2012). Traffic instabilities in self-organized pedestrian crowds. *PLoS Computational Biology*, 8(3), 1–10.
- Nakayama, A., Hasebe, K., & Sugiyama, Y. (2005). Instability of pedestrian flow and phase structure in a two-dimensional optimal velocity model. *Physical Review E*, 71, 036121.
- Parisi, D., & Patterson, G. (2017). Influence of bottleneck lengths and position on simulated pedestrian egress. *Papers in Physics*, 9, 090001.
- Predtechenskii, V. M., & Milinskii, A. I. (1978). *Planning for foot traffic flow in buildings*. New-Dehli, India: Amerind.
- R Core Team. (2014). R: A language and environment for statistical computing [Computer software manual]. Retrieved from <http://www.R-project.org/>
- Rumelhart, D., Hinton, G., & Williams, R. (1986). Learning representations by back-propagating errors. *Nature*, 323, 533–536. doi:10.1038/323533a0
- Sadati, N., & Taheri, J. (2002). Solving robot motion planning problem using Hopfield neural network in a fuzzified environment. Paper presented at the IEEE FS Conference (Vol. 2, pp. 1144–1149), Honolulu, HI.
- Schadschneider, A., Chraïbi, M., Seyfried, A., Tordeux, A., & Zhan, J. (2018). Pedestrian dynamics - From empirical results to modeling. In L. Gibelli & N. Bellomo (Eds.), *Crowd dynamics, volume 1. Modeling and simulation in science, engineering and technology*. Cham: Birkhäuser.
- Schadschneider, A., Klingsch, W., Klüpfel, H., Kretz, T., Rogsch, C., & Seyfried, A. (2009). Evacuation dynamics: Empirical results, modeling and applications. In R. A. Meyers (Ed.), *Encyclopedia of complexity and systems science* (pp. 3142–3176). New York, NY: Springer.
- Seyfried, A., Passon, O., Steffen, B., Boltes, M., Rupprecht, T., & Klingsch, W. (2009). New insights into pedestrian flow through bottlenecks. *Transportation Science*, 43(3), 395–406. doi:10.1287/trsc.1090.0263
- Shladover, S. E. (2018). Connected and automated vehicle systems: Introduction and overview. *Journal of Intelligent Transportation Systems*, 22(3), 190–200. doi:10.1080/15472450.2017.1336053
- Tordeux, A., Chraïbi, M., Seyfried, A., & Schadschneider, A. (2017). Data from: Prediction of pedestrian speed with artificial neural networks. Retrieved from <https://doi.org/10.5281/zenodo.1054017>
- Treiber, M., & Kesting, A. (2013). *Traffic flow dynamics*. Berlin: Springer.
- Weidmann, U. (1994). *Transporttechnik der Fußgänger* (Technical Report). ETH Zürich: Schriftenreihe des IVT Nr. 90.
- Zhang, J. (2012). *Pedestrian fundamental diagrams: Comparative analysis of experiments in different geometries* (Doctoral dissertation), Universität Wuppertal, Wuppertal. Retrieved from <http://juser.fz-juelich.de/record/128157>
- Zhang, J., & Seyfried, A. (2014). *Experimental studies of pedestrian flows under different boundary conditions*. Paper presented at the ITSC IEEE Conference (pp. 542–547), Qingdao, China.
- Zhang, Y., Xin, D.-R., & Wu, Y.-H. (2016). Pedestrian detection for traffic safety based on accumulate binary haar features and improved deep belief network algorithm. *Transportation Planning and Technology*, 39(8), 791–800.